Mapping long-term temporal change in imperviousness using topographic maps

James D Miller[a,*] & Stephen Grebby[b]

[a] Centre for Ecology and Hydrology, Benson Lane, Crowmarsh Gifford, Wallingford, Oxfordshire, OX10 8BB, UK

[b] British Geological Survey, Keyworth, Nottingham, NG12 5GG, UK

[*] Corresponding author: Tel: +44 (0)1491 692708; E-Mail: millj@ceh.ac.uk

Keywords: Imperviousness; Urban; Remote Sensing; Hydrology, Land Use Change

Abstract

Change in urban land use and impervious surface cover are valuable sources of information for determining the environmental impacts of urban development. However, our understanding of these impacts is limited due to the general lack of historical data beyond the last few decades. This study presents two methodologies for mapping and revealing long-term change in urban land use and imperviousness from topographic maps. Method 1 involves the generation of maps of fractional impervious surface for direct computation of catchment-level imperviousness. Method 2 generates maps of urban land use for sub-sequent computation of estimates of catchment imperviousness based on an urban extent index. Both methods are applied to estimate change in catchment imperviousness in a town in the South of England, at decadal intervals for the period 1960–2010. The performance of each method is assessed using contemporary reference data obtained from aerial photographs, with the results indicating that both methods are capable of providing good estimates of catchment imperviousness. Both methods reveal that peri-urban developments within the study area have undergone a significant expansion of impervious cover over the period 1960–2010, which is likely to have resulted in changes to the hydrological response of the previously rural areas. Overall, results of this study suggest that topographic maps provide a useful source for determining long-term change in imperviousness in the absence of suitable data, such as remotely sensed imagery. Potential applications of the two methods presented here include hydrological modelling, environmental investigations and urban planning.

1. Introduction

Accurate estimates of impervious surface coverage (commonly known as imperviousness) within watersheds (catchments) are required for hydrological modelling and urban land use planning because increased imperviousness results in decreases in infiltration and soil storage capacities (Kidd and Lowing, 1979). Furthermore, replacement of natural drainage with artificial conveyance pathways can also reduce catchment response times (Packman, 1980). These impacts can subsequently combine to increase the frequency and magnitude of flood events through increased and more rapid runoff (Huang et al., 2008; Villarini et al., 2009), and lead to disruption of natural groundwater recharge (Shuster et al., 2005; Im et al., 2012). Moreover, the hydrological alterations caused by increasing imperviousness typically give rise to environmental issues, such as degraded water quality, decreased biodiversity in water bodies, and increased stream-bank erosion (Schueler, 1994; Arnold and Gibbons, 1996; Hurd and Civco, 2004; Amirsalari et al., 2013). Such impacts can be especially pronounced in peri-urban developments; areas surrounding existing towns, which convert previously permeable rural land into highly impermeable and artificially drained catchments (Tavares et al., 2012).Understanding and modelling the long-term hydrological impacts of increased urban development requires concurrent information on the change in impervious surface coverage. Maps of impervious surfaces can be produced from either field surveys, manually digitising from hard-copy topographic maps, or the use of remote sensing (RS) data. Whereas field surveys and manual digitisation can be time-consuming and laborious, the large continuous areal coverage provided by RS datasets can be exploited using image processing algorithms to rapidly map impervious surfaces for only a fraction of the time and cost. Accordingly, RS is becoming increasingly recognised as a valuable tool for mapping imperviousness. A comprehensive, authoritative review of the different methodologies employed to map impervious cover from RS data is provided by Weng (2012). To summarise, RS-based approaches to mapping imperviousness generally fall into three broad categories: per-pixel, object-based and sub-pixel. Per-pixel approaches commonly involve producing a binary map by determining whether individual image pixels correspond to either pervious or impervious surfaces, typically through aggregating the classes of an initial land cover classification (Yuan and Bauer, 2006; Im et al., 2012; Amirsalari et al., 2013). In contrast, object-based approaches involved the classification of groups of contiguous image pixels (i.e., objects or regions) by also considering various shape, contextual and neighbourhood information (Benz et al., 2004; Weng, 2012). Classifying an image based on objects helps to overcome the "speckled" effect often encountered with per-pixel classification in urban areas (Van de Voorde et al., 2003), thus enabling improved mapping results (Yuan and Bauer, 2006; Zhou and Wang, 2008). A major limitation of per-pixel approaches is that they assume each pixel comprises a single land use or land cover type. However, pixels containing a mixture of land use or cover types are common in low-to-moderate resolution imagery acquired over complex heterogeneous landscapes such as urban areas (Weng, 2012). Sub-pixel approaches can be used to overcome this to derive accurate estimates of imperviousness because they decompose the pixel spectra into their constituent parts, therefore providing fractional measures of impervious surface area. Popular approaches in this category include unmixing the pixel spectra to determine the fractional abundance of each constituent end-member surface type (Lu et al., 2006), or modelling fractional imperviousness through statistical regression and scaling of spectral vegetation indices (Bauer et al., 2004; Van de Voorde et al., 2011).With the earliest source of RS data comprising panchromatic aerial photograph lacking in sufficient spectral information, the mapping of imperviousness using RS is restricted to the last few decades since the emergence of spectral satellite imagery (e.g., Landsat). Consequently, few studies have assessed long-term land cover change using RS data (e.g., Gerard et al., 2010; Tavares et al., 2012), and even fewer have mapped long-term changes in impervious cover (Weng, 2012). Therefore, our understanding of the hydrological impact and non-stationary flooding trends in relation to impervious surface change is somewhat limited (Ogden et al., 2011; Vogel et al., 2011; Dams et al., 2013). Linking imperviousness to alternative sources of digital geo-information could provide a means of mapping long-term changes in impervious cover. However, such datasets are not usually available at the national scale or comparable over long periods of time. National land cover mapping products such as the UK Land Cover Map (LCM) 1990, 2000 and 2007 (Centre for Ecology and Hydrology) cover only a short time period and are inconsistent due to the different processing algorithms applied to derive each product from the RS data (Morton et al., 2011). While methods such as land use trajectory analysis (Verbeiren et al., 2013) could be applied to help improve the consistency of the time-series somewhat, there will still likely be a residual error arising from the use of contrasting algorithms for generating each data product. Physical settlement boundaries and land use change statistics may be a useful alternative source of information (e.g., Bibby, 2009) but can only be loosely regarded as proxies for imperviousness. In most cases, the only consistent and long-term sources are topographic maps produced by national agencies. Within the UK topographic maps have been produced by the Ordnance Survey — the national mapping agency for Great Britain — since the mid-19th century. Despite representing a potentially valuable source for deriving long-term change in land use or land cover, studies assessing the use of such information are scarce (e.g., Hooftman and Bullock, 2012). The aim of this study is to utilise historical topographic maps for semi-automated mapping of urban land use change and change in impervious cover. Two novel methods are presented that utilise topographic maps to: (i) derive maps of fractional impervious surface for direct computation of catchment-level imperviousness; (ii) derive maps of urban land use for subsequent computation of estimates of catchment-level imperviousness based on an urban extent index. Impervious surface cover estimates computed using these two methods are validated using reference data generated through a RS-based image classification of high-resolution aerial photographs. The methods presented herein are employed in an attempt to determine their suitability for indicating change in urban land use and imperviousness — here throughout a 50-year period from 1960 to 2010 in a number of hydrological catchments surrounding a UK town that exemplifies rapid peri-urban development.

2. Study area

The study area (Fig. 1) encompasses two adjacent small urban stream catchments located to the north of Swindon in the south of England; comprising the Haydon Wick brook and Rodbourne stream, both tributaries of the River Thames (Fig. 1 inset). Swindon was designated as an Expanded Town under the Town Development Act in 1952 which encouraged town development in county districts to relieve over-population elsewhere. The Rodbourne stream catchment has been highly urbanised since the 1950s and comprises a large area of commerce and industry on the northern edge of Swindon town, along with highly urbanised housing developments. The Haydon Wick brook catchment is located further to the north of Swindon and has undergone widespread development since the 1990s, prior to which it was a predominantly agricultural landscape. Within the Haydon Wick catchment a number of distinct catchments (1–5) have been selected (Fig. 1) that capture and reflect the diversity and age of different developments within the area. The Rodbourne catchment, in which development has incrementally expanded since the 1950s, remains one single catchment unit (6) for this study. The focus of this study is to test two methodologies for mapping changes in urban land use and associated imperviousness in each of these six catchments during the period 1960 to 2010.3.

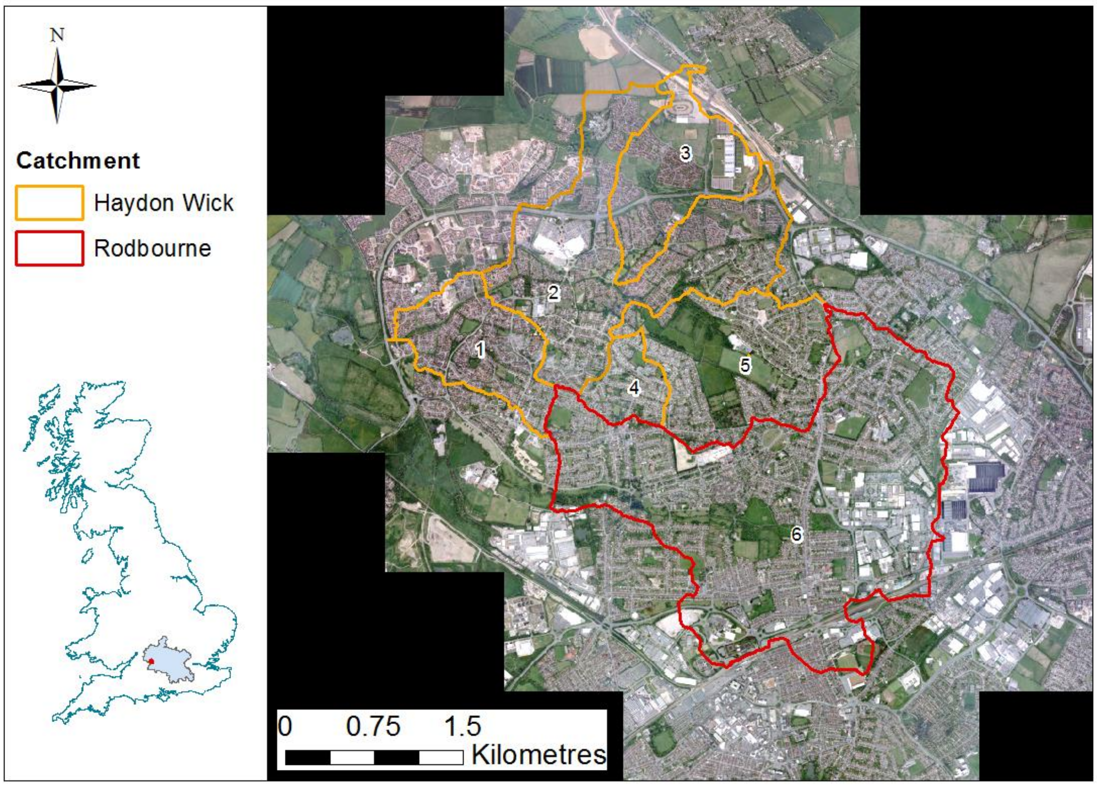

Fig. 1. Map of the study area showing catchment boundaries and location of the study area within the Thames Basin (inset). RGB aerial photography – © UK Perspectives: License Number UKP2006/01.

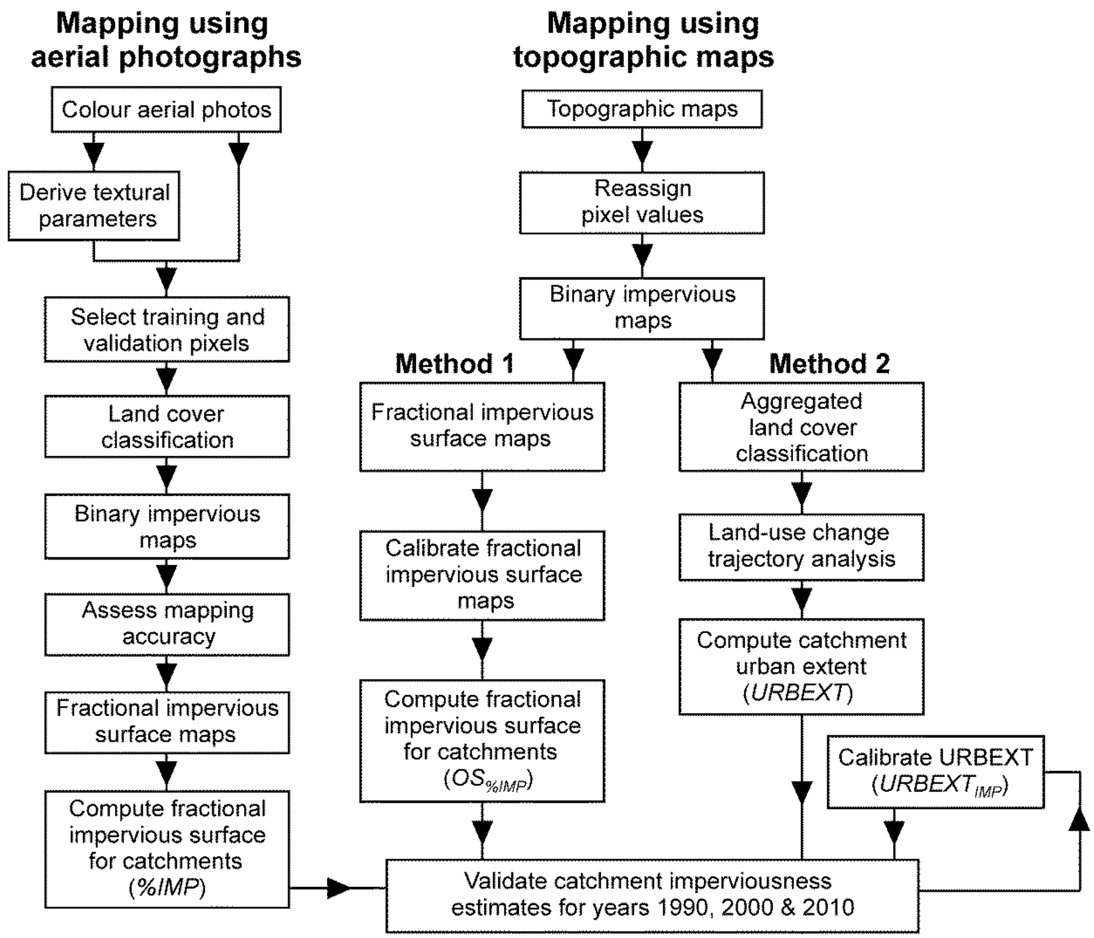

Fig. 2. Overview of methodological approach used to assess the utility of traditional topographic maps for long-term, historical mapping of urban extent and estimation of catchment imperviousness.

3. Material and methods

The ability to utilise traditional topographic maps for long-term, historical mapping of urban extent and estimation of catchment imperviousness is assessed using a three-pronged approach (Fig. 2). The approach involves first estimating contemporary catchment fractional impervious surface area directly from aerial photographs for use as reference data. These reference data are then used to validate the two methods presented in this paper for mapping historical change in impervious cover topographic maps. Following validation, a comparison of the two methods is undertaken to assess their relative performance revealing long-term change in catchment impervious cover between 1960 and 2010. More detailed information regarding the methodological approach is provided in the following sub-sections.

3.1 Deriving catchment imperviousness from aerial photographs

Reference data for quantifying the catchment fractional impervious cover were obtained from aerial photographs for three decadal time-slices within the 50-year period of interest — namely 1991, 1999 and 2010 (herein referred to as 1990, 2000 and 2010, respectively). The reference data were generated by first classifying 0.5 m true-colour aerial photographs into pervious land cover classes: grass, trees, bare soil and water; and impervious land cover classes: roads/pavements, commercial buildings and residential buildings. It was anticipated that land cover classes such as bare soil and roofing tiles could be particularly difficult to discriminate using the limited spectral information contained in only the red, green, blue bands of the aerial photographs. Therefore, textural information was also incorporated in the form of the Grey-Level Co-occurrence Matrix (GLCM) parameters of entropy, dissimilarity, second moment and homogeneity (Haralick et al., 1973; Herold et al., 2003). These parameters were derived from the green band in the ENVI 4.8 software package (Research Systems, Inc.) for a 3 × 3pixel (i.e. 1.5 m × 1.5 m) window and a co-occurrence window shift of 4 pixels (i.e., 2 m) in both the x- and y-direction. This combination of window size and shift was chosen as it maximised visual discrimination of the different land cover classes. Classification of the three time-slices employed a neural network (NN) classification algorithm in conjunction with the seven associated spectral and textural bands. A NN classifier was chosen because they are capable of producing better classification results for complex heterogeneous urban areas than their conventional counterparts (e.g., Maximum Likelihood), since they are non-parametric and more robust in handling noisy and non-normally distributed data (Foody, 2002). The NN used in this case was a Multi-Layered Perceptron NN with a back-propagation learning algorithm for supervised learning (Richards and Jia, 2006). Using a three-layered NN (i.e., input, output and one hidden layer), land cover classifications were performed in ENVI 4.8 with the default training parameters confirmed through a set of trial-and-error experiments. Each classification was supervised with the aid of a set of training pixels that were carefully selected in the imagery to represent each of the defined land cover types (~6000 pixels for each class). Land cover classifications were converted to binary imperviousness maps by collapsing the classes into just two corresponding to pervious or impervious surfaces (Yuan and Bauer, 2006; Im et al., 2012; Amirsalari et al., 2013). The accuracies of the resulting binary imperviousness maps were determined by comparing the true class identities of a sample of validation pixels to the classes assigned through classification. Validation pixels were selected from regions of interest (ROIs) of known pervious or impervious surface class identities that were defined in each time-slice image based on extensive knowledge of the study area. Validation pixels were then selected from the ROIs using a random stratified sampling protocol to ensure each class was represented proportionately, and to avoid spatial autocorrelation within the validation dataset (Chini et al., 2008; Pacifici et al., 2009). The minimum validation sample size required to derive statistically valid accuracy estimates for the entirety of each binary map was determined from the normal approximation of the binomial distribution (Fitzpatrick-Lins, 1981). Consequently — based on an expected accuracy of 50% and a precision of ±0.5% at the 95% confidence level —

approximately 19,000 validation pixels for each class were selected to determine the accuracy of each binary imperviousness map.

Binary imperviousness map accuracies were assessed by way of the overall (OA), user's (UA) and producer's (PA) accuracies and the Kappa coefficient (K) derived from a confusion matrix (Congalton, 1991). The overall accuracy is the percentage of all validation pixels correctly classified, whereas the user's and producer's accuracies provide information regarding the commission and omission errors associated with the individual classes, respectively. Following validation, the 0.5 m binary impervious maps were aggregated to 50 m grid cells to generate fractional impervious surface maps, with the value for each grid cell corresponding to the proportion of impervious pixels within it. The value of 50 m was selected as it was found to best represent homogeneous scale of urban land use classification (see Section 3.2.2). The imperviousness of each of the six catchments (*%IMP*) was then computed from these fractional impervious surface maps for use as reference data, using:

$$\%IMP = \frac{\sum_{i}^{n}\left(\%IMP_i \times A_i\right)}{A_c}, \quad (1)$$

where $\%IMP_i$ is the fractional impervious cover for grid cell i, A_i is the area of the grid cell, n is the number of grid cells within the catchment, and A_c is the total catchment area.

3.2 Deriving estimates of catchment imperviousness using topographic maps

As outlined in Fig. 2, estimates of catchment fractional impervious surface cover were derived using two methods. In general, these consist of first generating binary imperviousness maps from the topographic maps and then computing catchment imperviousness from either fractional imperviousness maps or urban land use maps — as illustrated in Fig. 3 and described below.

3.2.1 Data and pre-processing

Digital historical topographic maps produced by the UK Ordnance Survey (OS) between 1960 and 2010 were obtained in raster format as 25 km × 25 km tiles with a 1 m spatial resolution. For each decade (1960s to 2010s), the most contemporaneous map tiles produced for that decadal time-slice were obtained and mosaicked to produce a seamless image for each decade (Table 1). The primary step for the two methods is to convert the historical topographic maps into simplified and physically representative binary maps of developed (i.e., impervious) and undeveloped (i.e., pervious) pixels. To do this, the original pixel values were reclassified so that a value of 1 was assigned to pixels corresponding to 'white space' on the map and a value of 2 to all pixels corresponding to mapped features.

Table 1. Ordnance Survey mapping data and pre-processing requirements.

Decade and period of coverage	Format	Spatial Resolution	Pre-aggregation processing requirements for binary maps
1960 (1960-1961) 1970 (1967-1978) 1980 (1984-1987) 1990 (1990-1992)	Scanned and geo-referenced black & white 'colormap' raster	1m	Mosaicking tiles → reclassification to integers → removal of forest detail and cartographic information → infill of industrial areas
2000 2010	Digital geo-referenced black & white integer raster	1m	Mosaicking tiles → infill of large buildings, commercial and industrial areas → removal of cartographic information

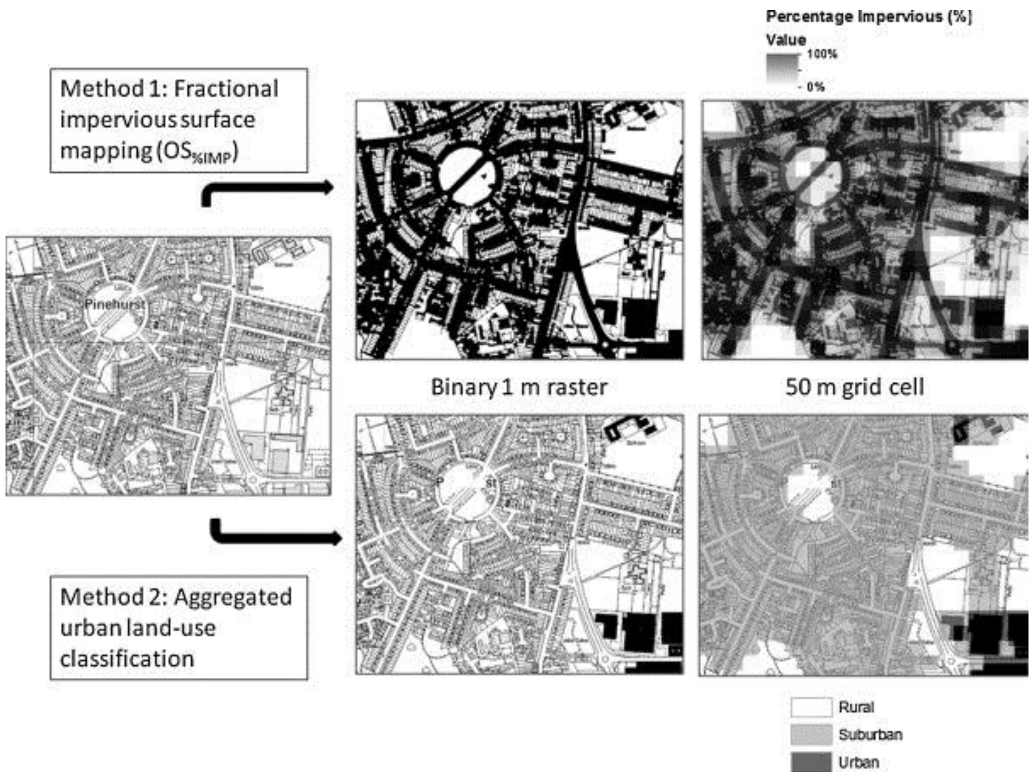

Fig. 3. Illustration of the approach applied in both method 1 and 2 to map impervious cover. Topographic base map – © Crown copyright and Landmark Information Group.

Due to slight variations in the cartographic style used from 1960 to 2010, a number of steps were required to further improve the consistency and compatibility of each map. The first stage involves developing 'level-1' binary maps, in which artefacts and key inconsistencies between maps from each decade are reduced. This was undertaken using the 'Raster Cleanup' tool in ArcMap (ArcGIS 10, ESRI) and included the following steps:

- A rapid 'clean-up' of each raster map is undertaken to remove features, such as place names or symbols relating to widespread forest;
- Reclassifying large concrete or tarmac areas represented by 'white space' to developed areas;

- Infilling the roofs of large buildings on raster maps for 2000–2010due to the low density of pixels used to represent such areas on these maps.

A second pre-processing stage was subsequently applied for the purpose of infilling developed features such roads and buildings to generate a set of ‘level-2’ binary maps. This was undertaken in ArcMap by applying the ‘Boundary Clean’ tool to each raster and then converting them to polygon shapefiles. This conversion enables road segments and buildings to be readily reattributed to alter them from polygons representing pervious (undeveloped) features to impervious (developed) features. Once all relevant polygons have been reassigned, the shapefiles were then converted back to raster format.

3.2.2 Deriving catchment imperviousness from fractional impervious surface maps

The first method (method 1) for deriving catchment imperviousness for the six catchments is relatively straightforward to implement, and is focussed on the generation of fractional impervious surface maps of the study area. To generate these maps, the ‘level-2’ binary maps derived from the topographic maps were aggregated to 50 m grid cells in a similar manner to that used to derive fractional impervious surface maps from the aerial photographs. In this case, the value for each 50 m grid cell is calculated as the proportion of 1 m impervious pixels contained within it. Although pre-processing steps were implemented to improve the compatibility and consistency of the topographic map time series (1960–2010), additional calibration was performed to account for any residual discrepancies between the fractional impervious surface maps. Adopting the approach outlined by Lu et al. (2011), pseudo-invariant pixels (i.e., those remained unchanged in terms of imperviousness throughout the time series) were selected for pair-wise image calibration via linear regression models. As a result, all fractional impervious surface maps were calibrated to the most recent map (i.e., 2010). Once calibrated, the imperviousness of each of the six catchments ($OS_{\%IMP}$) is computed from these calibrated fractional impervious surface maps using an adaptation of Eq. (1), and compared with the contemporaneous reference data derived from aerial photography (*%IMP*).

3.2.3 Deriving catchment impervious cover from urban land use maps

The second method (method 2) for deriving catchment imperviousness for the six catchments is based on the generation of urban land use maps from the topographic maps. Maps of urban land use were generated by aggregating the topographic map-derived binary maps for each decade to larger grid cells, and then classifying the cells according to the LCM land use/land cover definitions; mixed development and green space designated as Suburban (e.g., houses with gardens), areas of near continuous development with little vegetation (e.g., industrial estates) designated continuous Urban (Fuller et al., 2002), and all other areas of green and general pervious surfaces referred to as Rural. Following a preliminary evaluation of a number of different grid cell sizes, a cell size of 50 m was identified as the optimum for generating realistic, homogeneous urban land use maps; smaller cell sizes produced maps with the aforementioned 'speckled' effect that often affects per-pixel classification in urban areas. Additionally, it was found that application of this approach to the 'level-2' binary grids resulted in difficulty devising a standard classification which can be used to produce coherent land use maps across the time series. For this reason, the 'level-1' binary maps derived from the topographic maps were used to generate the land use maps. This was achieved using ArcMap through the following steps:

- ‘Level-1’ binary maps were aggregated using the ‘Aggregate’ function to generate a grid that details the mean value of the pixels contained within each 50 m grid cell. These aggregated values provide an indication of the level of development; 50 m grid cells with a value close to 1 essentially correspond to ‘white space’ (i.e., a rural undeveloped area), whereas a value close to 2 corresponds to a high density of mapped features (i.e., a highly developed area).
- A threshold-based classification scheme was then applied to the grid in order to assign cells to either the Urban, Suburban or Rural land use class. It was found that cell values of 1–1.35 represented Rural land use, values of 1.35–1.65 corresponded to Suburban, and values above 1.65 represented Urban land use. These thresholds were validated to ensure at least 80% of 50 randomly selected grid cells were correctly classified in decadal map. The output is set of 50 m maps showing Rural, Suburban, and Urban land use (shown in Fig. 3).

Potentially erroneous pixel classifications were removed through geospatial proximity analysis, and by applying an urban land use change trajectory demonstrated by Verbeiren et al. (2013) to ensure greater consistency throughout the time series. This is achieved by first combining the ArcGIS ‘Conditional’ tool in the ‘Raster Calculator’ with the ‘Focal Statistics’ tool to identify misclassified Urban and Suburban grid cells based on the classes of neighbouring cells — isolated Suburban or Urban cells were reclassified according to the dominant surrounding class. Following this, each cell was labelled as either 0 (Rural), 1 (Suburban) or 3 (Urban) and all trajectories of land use change were recorded throughout the time series using codes (e.g., 00112, 01222, etc.). These were then evaluated according to whether they reflect realistic changes observed in the catchment over the study period, and subsequently classified into 6 rationality classes: 'urban growth', 'suburban growth', 'urban regeneration', 'urban stability', 'suburban stability', and 'inconsistent'. The 'inconsistent' class captures grid cells that do not follow realistic change trajectories — such as a Suburban area changing to Rural then Suburban and back to Rural. Inconsistent cells were corrected using the most likely trajectory for that cell over the 50-year period — based upon surrounding cells. The class 'urban regeneration' captures the possibility of Urban areas being demolished and replaced with green space or subsequent re-development. The land use change trajectory rules were implemented using the 'Conditional' tool in the ArcMap 'Raster Calculator'. The outcome was as set of coherent urban land use maps revealing the long-term change in land use for the period 1960–2010.

For each land use map, the proportions of Urban and Suburban grid cells within each catchment were used to calculate a catchment index of urban extent. As well as measuring the urban extent within a hydrological catchment, the index of urban extent (*URBEXT*) proposed in the UK Flood Estimation Handbook (FEH) methodology (Institute of Hydrology, 1999) can also provide an estimate of the impervious surface cover. Accordingly, the index of urban extent and estimate of imperviousness for the six catchments (*URBEXT*) in each land use map is computed using:

$$URBEXT = Urban + (\beta \times Suburban), \tag{2}$$

where *Urban* and *Suburban* are the proportions of Urban and Suburban grid cells within each catchment, respectively, and β is the Suburban weighting factor. The suitability of *URBEXT* for estimating catchment imperviousness is assessed through comparison with the reference data derived from aerial photography (*%IMP*). For the purpose of this comparison, *URBEXT* — the weighted value of urban extent within a catchment — is considered to provide a direct estimate of the catchment percentage imperviousness. The Suburban weighting factor (β) is preset to a value of 0.5 to account for the general equal mixture of built-up land and permanent vegetation (Bayliss et al, 2006; Institute of Hydrology, 1999). Urban land use was assigned a weighting of 1 because such areas generally have negligible green (pervious) space. In an attempt to improve the accuracy of the catchment imperviousness estimates, an optimal value for β was sought by applying a linear regression model between reference imperviousness (*%IMP*) and *URBEXT* across the three decadal time-slices. This provides a refined calibrated value of catchment impervious surface ($URBEXT_{IMP}$).

4. Results and discussion

4.1 Imperviousness maps from aerial photography

The accuracies of the RS-derived high-resolution (0.5 m) maps of binary imperviousness for 1990, 2000 and 2010 are shown in Fig. 4. High overall accuracies (>86%) were achieved in all three cases and are also confirmed by the corresponding K values (0.74–0.83); interpreted as reflecting a “substantial” to “almost perfect” degree of accuracy (Landis and Koch, 1977). Further corroboration of the classification accuracy is provided by the high user’s (88–99%) and producer’s (77–89%) accuracies associated with both the pervious and impervious classes in all binary imperviousness maps; indicating low commission and omission errors, respectively. The result of this accuracy assessment indicate that the binary imperviousness maps are suitable for deriving reference data for validating the estimates of catchment imperviousness computed using the topographic map-based methods.

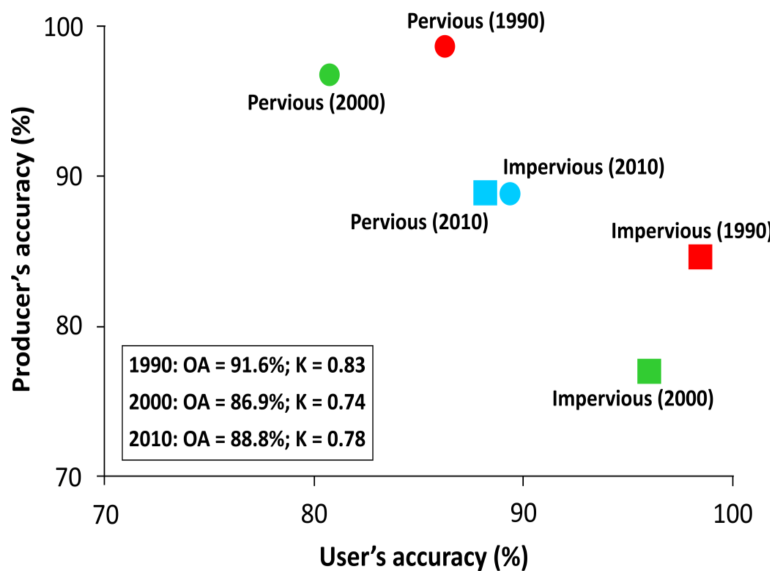

Fig. 4. Classification accuracies of the binary imperviousness maps derived from aerial photographs for 1990, 2000 and 2010. OA — Overall accuracy; K — Kappa coefficient.

4.2 Catchment imperviousness from fractional impervious surface maps

Catchment imperviousness obtained from topographic map-derived fractional impervious surface maps (*OS%IMP*) — method 1 — was compared with the reference data (*%IMP*) derived from the aerial photographs (Fig. 5). A reasonable, but variable level of agreement between *OS%IMP* and *%IMP* is observed throughout the three decadal time-slices. Although the correlation for 1990 is greatest (R^2 = 0.96), the catchment imperviousness measured using *OS%IMP* is (with the exception of catchment 3) approximately 10% larger than the reference data. The general overestimation of *OS%IMP* is most likely attributable to the larger size depictions of features such as roads on the 1990 topographic map, compared to equivalent features on the more recent maps. The correlation between *OS%IMP* and *%IMP* is somewhat lower for both 2000 and 2010 (R^2 = 0.75 and 0.62, respectively), with the data appearing more widely distributed around the reference *%IMP*. This observed decrease in the level of agreement could be due a slight offset in the exact instant in time at which the aerial photographs and corresponding topographic maps capture. Alternatively, this could arise due to the slightly lower accuracies of the 2000 and 2010 aerial photography-derived binary imperviousness maps, in comparison to the 1990 map. Nevertheless, the results suggest that estimating catchment imperviousness using fractional impervious surface maps derived from topographic maps (i.e., method 1) is feasible.

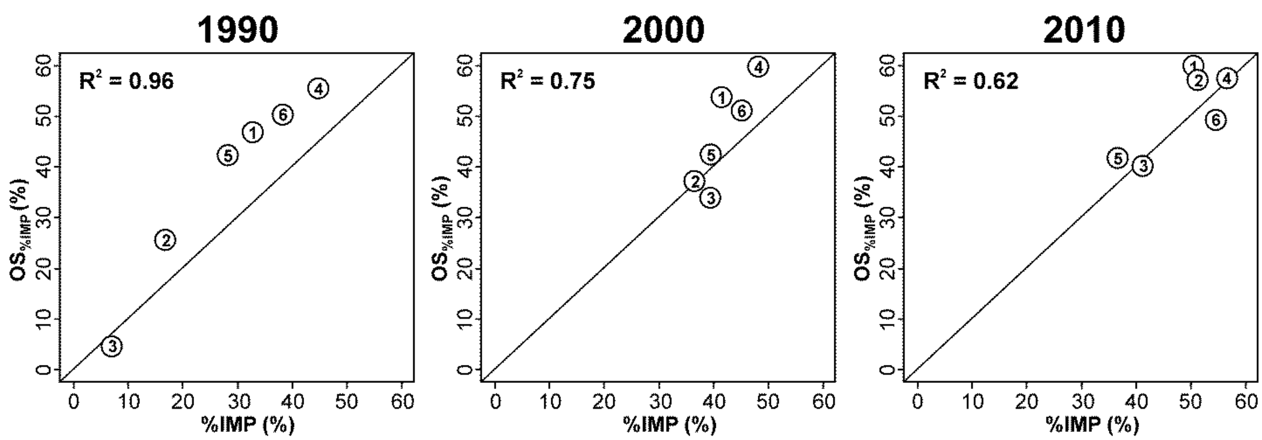

Fig. 5. Comparison of catchment imperviousness estimated from aerial photography *(%IMP*) and topographic map-derived fractional impervious surface cover (*$OS_{\%IMP}$*) within the six catchments, for years 1990, 2000 and 2010.

4.3 Mapping urban land use change using topographic maps

Urban land use derived from the topographic maps using method 2 reveals the spatio-temporal change in Urban, Suburban and Rural land use at a decadal intervals from the 1960s to 2010s (Fig. 6). While the highly urban Rodbourne catchment (catchment 6) exhibits a gradual expansion and infilling of Urban and Suburban land use, the Haydon Wick catchments (1–5) exhibit a more dramatic and rapid changes in land use over the 50-year study period. The remarkable change from predominantly Rural (agricultural) land use in all Haydon Wick catchments (1–5) to predominantly Suburban land use is clearly illustrated in Fig. 7, as is the impact of one large commercial development in catchment 2 in the 2000s. The relative change that occurred in catchment 6, which was already over 50% Suburban in 1960, is significantly less than in the peri-urban area of the Haydon Wick catchments (Fig. 7). In all cases, the mapped spatio-temporal changes in Urban land use were found to be consistent with the physical changes observed in the original OS topographic maps. By the 2010s, the relative proportion of developed (i.e., Urban or Suburban) land across all catchments is high and the remaining Rural areas typically represent areas of green space designated for recreation and conservation, along with areas of significant flood risk.

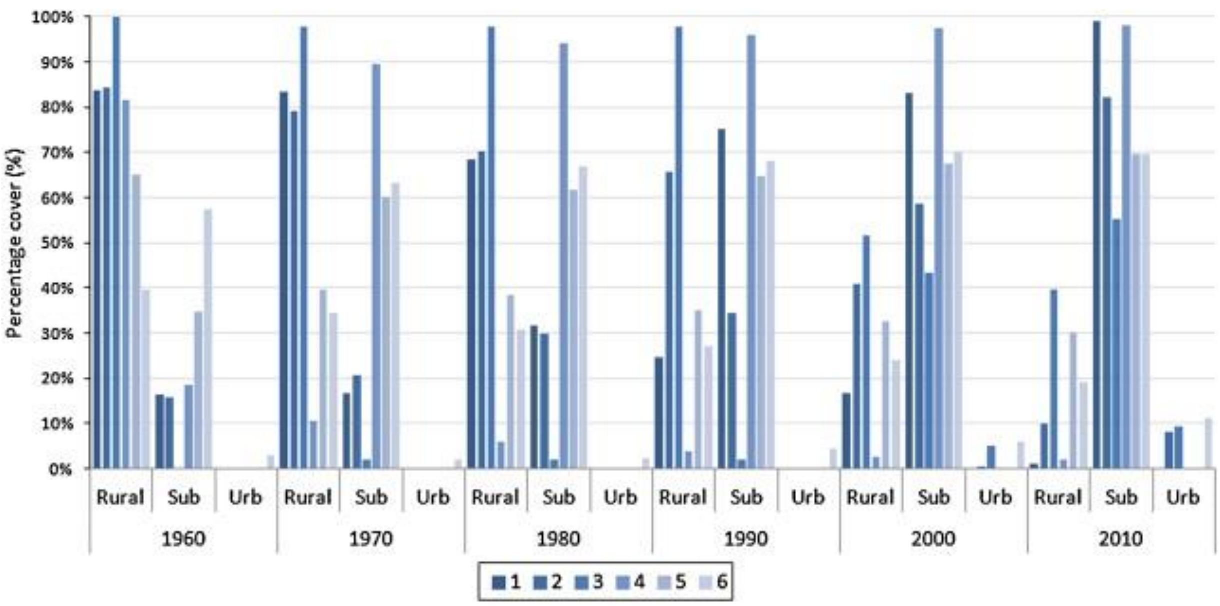

Fig. 6. Decadal change in land use across the study area catchments.

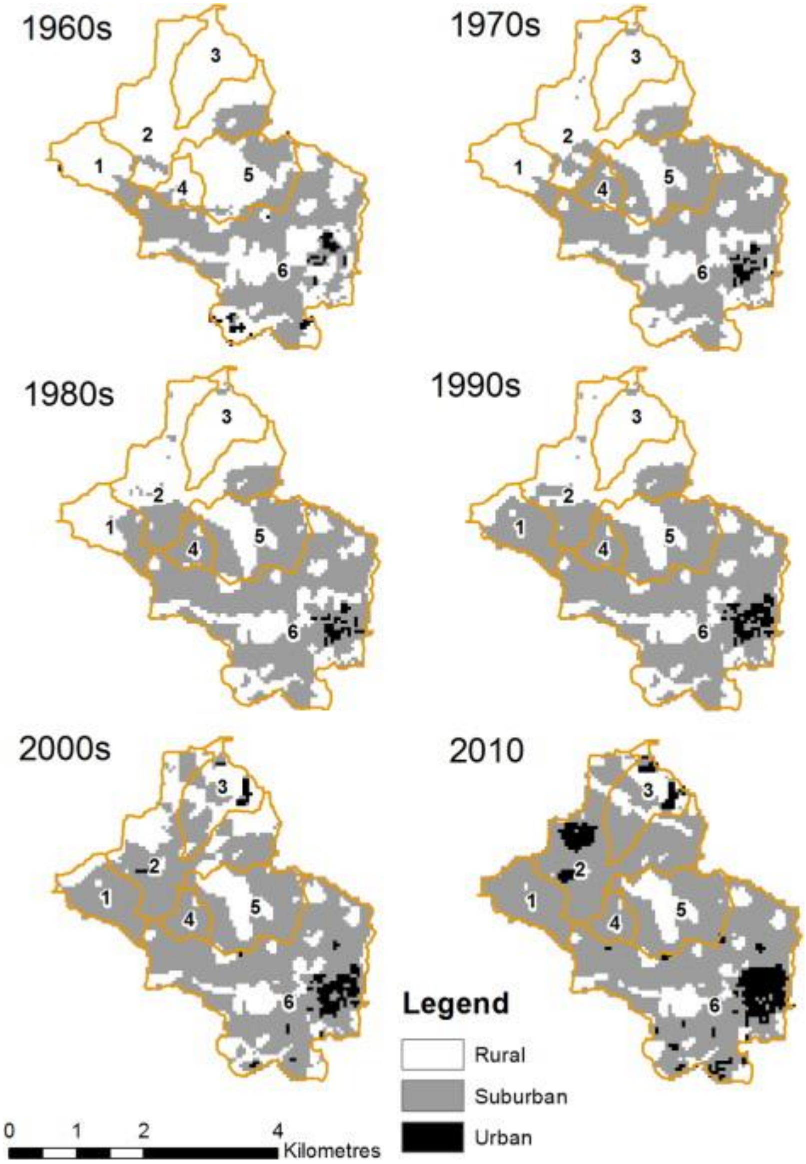

Fig. 7. Spatio-temporal change in urban land use across the study area.

Table 2. Change in urban extent index (*URBEXT*) for the six catchments.

Catchment	1960	1970	1980	1990	2000	2010	Percentage change (1960–2010)
1	8.2%	8.3%	15.8%	37.6%	41.6%	49.5%	41.3%
2	7.9%	10.4%	14.9%	17.2%	29.7%	49.2%	41.3%
3	0.0%	1.1%	1.1%	1.1%	26.8%	36.9%	36.9%
4	9.2%	44.7%	47.0%	48.0%	48.7%	49.0%	39.8%
5	17.4%	30.1%	30.8%	32.4%	33.7%	34.9%	17.5%
6	31.7%	33.7%	35.8%	38.7%	41.0%	45.9%	14.2%

Catchment values of *URBEXT* computed using the land use maps (Table 2) also show distinct differences between the Haydon Wick catchments (1–5) and Rodbourne catchment (6). During the period 1960–2010, URBEXT values changed little across the Rodbourne catchment, with only a 14.2% increase as a result of small, steady incremental change during each decade. More significant change across the Haydon Wick catchments reflects successive waves of peri-urban development during the study period, with an average overall increase in *URBEXT* of 35.4% and significant variation between the catchments (17.5–41.3%). Again, the observed temporal changes in urban extent were found to be consistent with known physical changes that occurred within the period 1960–2010. Therefore, the results demonstrate that the employed method is an effective approach for readily mapping long-term basic land use change and associated catchment-level urban extent from historical topographic maps. A particular important stage in this methodology is the application of land use trajectory analysis (e.g., Verbeiren et al., 2013), which was crucial in ensuring a reliable time series dataset from which only genuine land use change is revealed.

4.4 Catchment imperviousness from urban land use maps

To investigate whether a simple index of urban extent (*URBEXT*) derived from topographic maps can provide representative estimates of catchment imperviousness, a comparison with reference imperviousness derived from aerial photography (*%IMP*) was undertaken (Fig. 8). Overall, a high correlation between *URBEXT* and *%IMP* is observed across most catchments during the three decades (R^2 = 0.80–0.96), and also when all data is considered collectively (R^2 = 0.86). Nevertheless, some notable deviations were observed for specific catchments and time-slices. For example, values of *%IMP* for catchment 3 were shown to be much higher than URBEXT in all cases due to significant underestimation of Urban areas of gravel and tarmac because of their depiction on topographic maps. Also, for 1990, URBEXT values are clustered around *%IMP*, while *URBEXT* consistently underestimates catchment imperviousness for both 2000 and 2010. The general underestimation of catchment imperviousness is likely to relate to the use of the 'level-1' binary grids, in which buildings and roads are not infilled. Nonetheless, it is apparent that land use maps generated from topographic maps can be used in conjunction with the urban index, *URBEXT*, (i.e., method 2) to generate feasible estimates of catchment imperviousness.

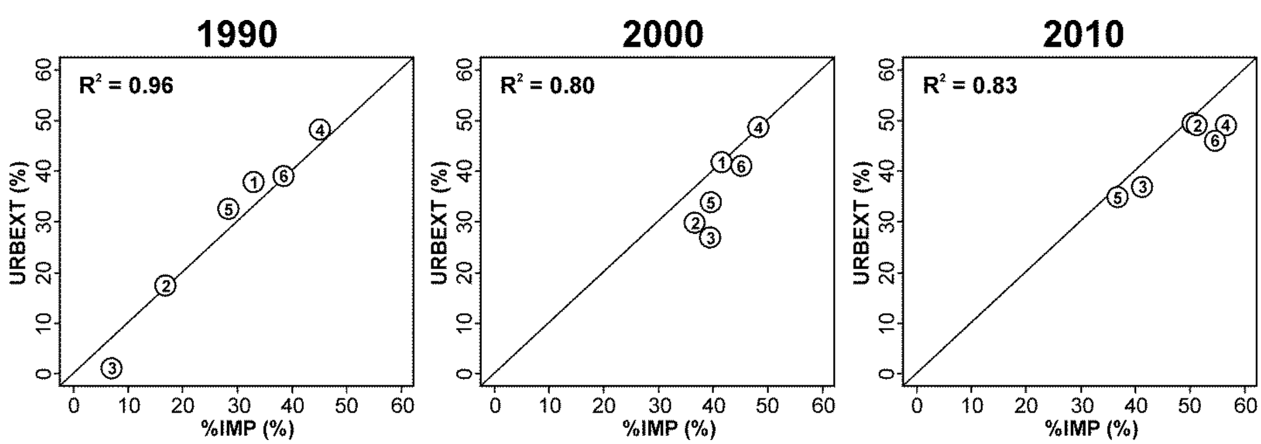

Fig. 8. Comparison of catchment imperviousness estimated from aerial photography *(%IMP)* and topographic map-derived index of urban extent (*URBEXT*) within the six catchments, for years 1990, 2000 and 2010.

A linear regression model between *URBEXT* and *%IMP* across the three decadal time-slices returned an optimised Suburban weighting factor (β = 0.53). Calibrated values of urban extent ($URBEXT_{IMP}$) for each catchment were computed for 1990, 2000 and 2010 by using this optimised value for β in Eq. (2). Following a comparison, the overall correlation between $URBEXT_{IMP}$ and %*IMP* (R^2 = 0.84) was actually found to be marginally lower than for *URBEXT* (R^2 = 0.86), indicating that the original preset β (0.5) was more appropriate in this particular case. However, in regions where Suburban land use does not comprise equal mixtures of built-up land and vegetation, the optimal weighting can be determined using the same approach as that used here.

4.5 Historical change in imperviousness

The two methods employed in this paper for computing catchment imperviousness from topographic maps both provide a means of revealing long-term change in imperviousness. As illustrated by Fig. 9, the overall trend in imperviousness change for 1960–2010 is consistent between the two methods. With the exception of catchment 6, which was already highly developed prior to 1960, all catchments experience a somewhat rapid increase in imperviousness during a specific period between 1960 and 2010. For example, catchment 1 sees its biggest increase in imperviousness during 1980–1990, while catchment 3 experiences a rapid rise during 1990–2000. The timings of these rapid increases in imperviousness coincide with known episodes of peri-urban expansion within the study area, and reflect the pattern of continuous growth and expansion where as one development finishes another one commences. The less dramatic change observed for catchment 5 can be explained by the fact that it already contained suburban housing stock in 1960 and that it also contains a large nature reserve which is protected from development.

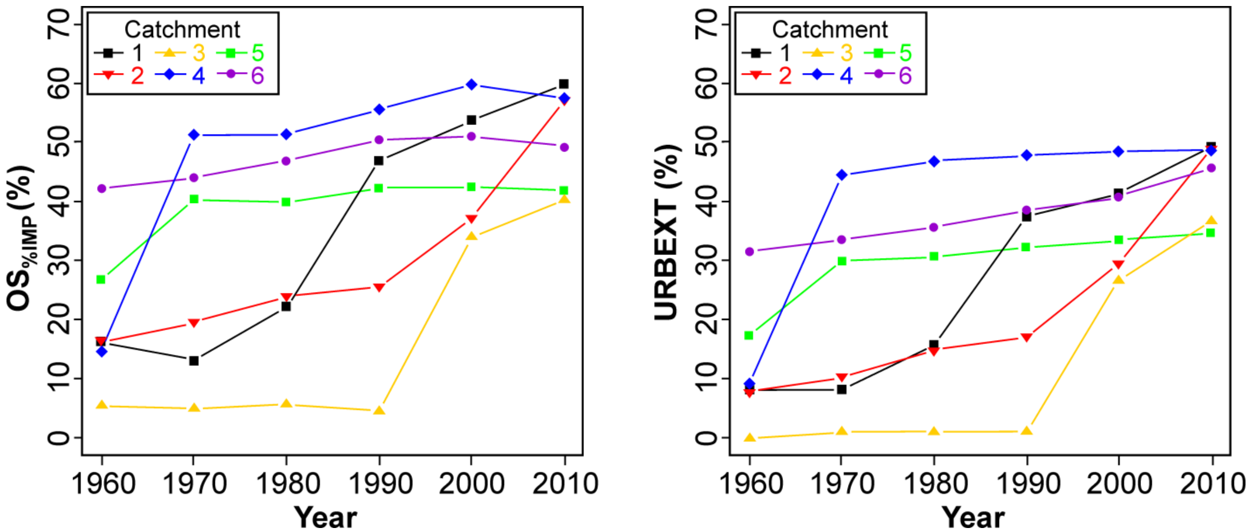

Fig. 9. Change in impervious cover determined using two methods across the six study catchments (1960–2010).

In addition to displaying similar trends, the two methods provide very similar estimates of the total absolute change in catchment imperviousness between 1960 and 2010. The mean difference in the total absolute change estimates between the two methods, for all catchments, is 2.9%, with individual catchment estimates varying between a maximum difference of 7.1% and a minimum of 0.4%. The maximum difference is associated with catchment 6, which is arguably the most complex in terms of land use change during 1960–2010 because of gradual expansion of the industrial area in the south-eastern section of the catchment, and regeneration of the railway network to suburban housing in the south-west. As illustrated by Fig. 9, the more rural northern catchments (i.e., 1–4) experienced the most significant total absolute change in catchment impervious across the entire study period, with increases of between 36% and 42%.

These estimates clearly reflect the rapid expansion of suburban land use into these previously rural areas as revealed in Fig. 6.

Although Fig. 9 illustrates that the methods reveal similar trends and estimates of change in imperviousness across the six catchments for 1960–2010, there are differences in the individual catchment imperviousness estimates. Specifically, all estimates computed using method 1 ($OS_{\%IMP}$) exceed those produced using method 2 (*URBEXT*), with a mean absolute difference of 7.8% (Table 3). With respect to the time intervals, the largest differences between the methods occurs for the years 1990 and 2000,where $OS_{\%IMP}$ estimates are respectively 8.3% and 9.4% greater than the equivalent URBEXT estimates. With respect to catchments, the largest differences between methods are observed for catchments 5 and 6, for which $OS_{\%IMP}$ estimates are respectively 9.0% and 9.5% greater than URBEXT estimates. The overall trend of method 1 producing higher estimates than method 2 is explained by a combination of the contrasting representation of features such as roads and buildings in the different binary maps (i.e., the level of infilling) incorporated in the two methods, and the somewhat simplistic discrete weighting system employed in method 2. In particular, the infilling of features such as roads in the level 1 binary maps used in method 1 can lead to overestimation of impervious cover as the symbology used represent roads does not always reflect the true physical dimensions, and can lead to infill of isolated areas that are not physically developed. Despite the fundamental differences in the two methods, both have been demonstrated to be feasible approaches for computing catchment imperviousness and its historical change from topographic maps.

Table 3. Absolute difference (*$OS_{\%IMP}$* – *URBEXT*) in estimates of imperviousness cover using two topographic map-based methods.

Year	1	2	3	4	5	6	Mean difference
1960	8.0	8.2	5.5	5.4	9.3	10.4	7.8
1970	4.7	9.1	3.8	6.4	10.2	10.3	7.4
1980	6.3	9.0	4.6	4.3	9.0	11.1	7.4
1990	9.2	8.3	3.4	7.5	9.8	11.6	8.3
2000	12.0	7.4	7.1	11.0	8.7	10.0	9.4
2010	10.3	7.8	3.3	8.3	6.8	3.3	6.6
Mean difference	8.4	8.3	4.6	7.2	9.0	9.5	7.8

4.6 Considerations in using topographic maps for estimating imperviousness

This paper demonstrates, through two methods, that topographic maps can be used to compute estimates of catchment imperviousness. When contemplating the use, or evaluating the performance, of *$OS_{\%IMP}$* and *URBEXT* — or any other topographic map-based method — there are a several aspects that require some consideration:

I. Aerial photographs and topographic maps do not necessarily represent the exact same instant in time, since whereas aerial photographs provide a snapshot for a specific date, topographic maps incorporate updates within a given time period (see Table 1).

II. Failure to remove place names and symbols (e.g., to represent forests) from the topographic maps will translate to the subsequently derived binary maps and lead to a degree of overestimation of imperviousness – users should ensure some consistent criteria are outlined for any manual interventions.

III. Topographic maps do not readily discriminate areas of inland bare ground and concrete/tarmac features, which will subsequently lead to their misrepresentation on derived binary impervious surface maps and result in a degree of underestimation of imperviousness. However, infilling of features such as roads can lead to overestimation of impervious cover if the symbology used does not directly reflect true physical dimensions.

IV. Small-scale features (e.g., minor roads) and minor changes within existing development boundaries (e.g., infilling or 'urban creep') shown on aerial photography are not always captured using the discrete land use classification and scale employed in method 2.

V. Calibration of the fractional impervious surface maps (as in method 1) and implementation of land use trajectory analysis (method 2) are crucial steps in producing a coherent time series dataset for revealing reliable long-term change in imperviousness.

With both methods capable of providing good estimates of catchment imperviousness, the most appropriate method is largely dependent on the purpose of the study and the format of the topographic maps. In general, method 1 can be more readily implemented and provides maps of fractional impervious surfaces, thus describing imperviousness on a continuous scale (Fig. 10). On the other hand, despite method 2 providing only a discrete description of imperviousness (see Fig. 10), it does provide maps of general land use that are informative when interpreting changes in imperviousness over time. Although method 1 can be readily applied to any study area, as demonstrated here, method 2 can be calibrated to determine the optimal weighting factor associated with Suburban land use (β). Additionally, if the available topographic maps depict roads and building as infilled features (akin to the 'level-2' binary maps) then method 1 would be more suitable. However, if — as in the case of the OS topographic maps used here — such features are not infilled, then method 2 can be applied without the need of additional pre-processing steps to produce 'level-2' binary maps.

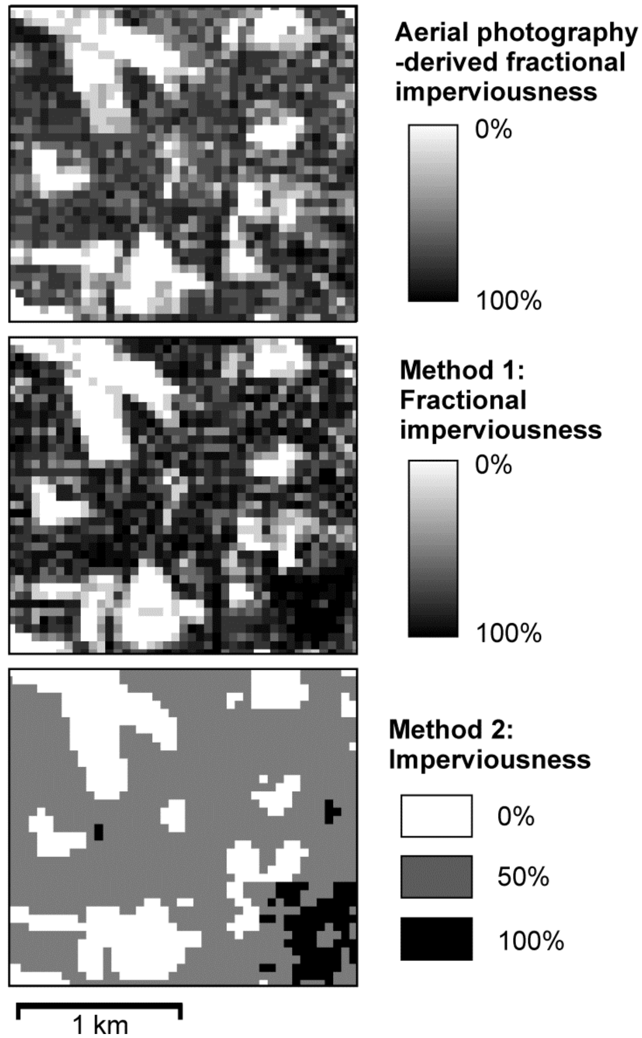

Fig. 10. A comparison of impervious surface maps obtained using the two methods.

5. Conclusions

This paper demonstrates that it is possible to derive robust long-term estimates of catchment imperviousness from topographic maps using two different contrasting methods. The first method (method 1) generates fractional impervious surface maps from the topographic maps and uses these to estimate catchment imperviousness. The second method (method 2) generates generalised land-use maps from the topographic maps and then computes catchment imperviousness from these using an index of urban extent. Although some degree of manual intervention is required for both methods, the processing stages employed are largely semi-automatic and require significantly less time than manual delineation of impervious surfaces. Such manual intervention will rely on some degree of user subjectivity — related to the format of the topographic maps — that could alter the binary map sand derived impervious cover products. Such interventions are required to produce more consistent mapping products for derivation of binary maps, and it is recommended that users employ transparency in the reporting of such interventions. Through comparison with reference data obtained using aerial photographs, it is demonstrated that both methods are capable of providing accurate estimates of catchment imperviousness and its change over time. With both methods capable of providing good estimates of catchment imperviousness, the most appropriate method beyond this study will be largely dependent on the purpose of the study and the format of the topographic maps.

This study demonstrates that both methods show the peri-urban Haydon Wick catchment has undergone a significant change from predominantly rural to highly urban and is now dominated by suburban areas of housing development. Findings from hydrological studies (e.g. Braud et al., 2012; Dams et al., 2013) would suggest that this will have led to a faster catchment response and greater magnitude of flow during storm events — making the area more prone to flooding. Local reports of more frequent flooding would are consistent with this hypothesis but hydrological modelling of the change in storm runoff response would be necessary to validate this assumption.

Several issues that may affect derived estimates of catchment imperviousness using topographic maps are highlighted for consideration in future applications of this methodology. For example, catchments containing large areas of concrete, gravel and tarmac (e.g., car parks) might not be recognisable as developed surfaces on topographic maps. Conversely, although such surfaces are typically characterised as impervious, they are not always physically impervious per se. For example, gravel cover is not inherently impervious and more modern car parks and roads can employ Sustainable Urban Drainage Systems (SUDS) design principles to enable infiltration of water to the media below. Furthermore, the presence and spatial distribution of both traditional drainage systems and SUDS contribute to the effective impervious area (EIA) — the connectivity to impervious areas — and are shown to be a strong determinant of storm runoff response (Han and Burian, 2009). This highlights the limitation of using simple impervious area estimates in hydrological studies. Also, depending on the maps scale, plot-scale (changes such as housing extensions driving urban creep; Perry and Nawaz, 2008) may not be captured on topographic maps.

Further research is required to progress to a more realistic scheme which accounts for varying degrees of imperviousness within individual land use or land cover classes. This would require better characterisation of urban typologies and land cover classes in terms of their natural permeability, association with drainage systems, and additional factors which affect the catchment runoff response. Such information would have to be obtained from auxiliary datasets as this is not readily available on historical topographic maps. Imperviousness maps incorporating information on connectivity and features that influence hydrological response to storm events would be particularly useful in quantifying the impact of historical urbanisation on flooding.

Acknowledgements

The authors would like to thank Thomas Kjeldsen and France Gerard of the Centre for Ecology and Hydrology and Rachel Dearden of the British Geological Survey for their contributions. We are also thankful to the two anonymous reviewers for their comments and suggestions, which helped to improve the quality of this manuscript. SG publishes with the permission of the Executive Director of the British Geological Survey (NERC).

References

Amirsalari, F., Li, J., Guan, X., & Booty, W. G. (2013). Investigation of correlation between remotely sensed impervious surfaces and chloride concentrations. *International Journal of Remote Sensing*, *34*, 1507–1525.

Arnold, C. L., & Gibbons, C. J. (1996). Impervious Surface Coverage: The emergence of a key environmental indicator. *Journal of the American Planning Association*, *62*, 243–258.

Bauer, M. E., Heinert, N. J., Doyle, J. K., & Yuan, F. (2004). Impervious surface mapping and change monitoring using Landsat remote sensing. *ASPRS Annual Conference Proceedings, Denver, Colorado, May 2004*.

Bayliss, A. C., Black, K. B., Fava-Verde, A., & Kjeldsen, T. R. (2006). URBEXT$_{2000}$ – A new FEH catchment descriptor: Calculation, dissemination and application. *Joint Defra/EA Flood and Coastal Erosion Risk management R & D Programme. R&D Technical Report FD 1919/TR*, (pp. 49).

Benz, U. C., Hofmann, P., Willhauck, G., Lingenfelder, I., & Heynen, M. (2004). Multi-resolution, object-oriented fuzzy analysis of remote sensing data for GIS-ready information. *ISPRS Journal of Photogrammetry and Remote Sensing, 58*, 239–258.

Bibby, P. (2009). Land use change in Britain. *Land Use Policy, 26*, S2–S13.

Braud, I., Breil, P., Thollet, F., Lagouy, M., Branger, F., Jacqueminet, C., Kermadi S, & Michel K. (2012). Evidence of the impact of urbanization on the hydrological regime of a medium-sized periurban catchment in France. *Journal of Hydrology*, *485*, 5–23.

Chini, M., Pacifici, F., Emery, W. J., Pierdicca, N., & Del Frate, F. (2008). Comparing statistical and neural network methods applied to very high resolution satellite images showing changes in man-made structures at rocky flats. *IEEE Transactions on Geoscience and Remote Sensing*, *46*, 1812–1821.

Congalton, R.G. (1991). A review of assessing the accuracy of classifications of remotely sensed data. *Remote Sensing of Environment*, *37*, 35–46.

Dams, J., Dujardin, J., Reggers, R., Bashir, I., Canters, F., & Batelaan, O. (2013). Mapping impervious surface change from remote sensing for hydrological modelling. *Journal of Hydrology*, *485*, 84–95.

Fitzpatrick-Lins, K. (1981). Comparison of sampling procedures and data analysis for a land-use and land-cover map. *Photogrammetric Engineering and Remote Sensing, 47,* 343–351.

Foody, G. M. (2002). Hard and soft classifications by a neural network with a non-exhaustively defined set of classes. *International Journal of Remote Sensing*, *23,* 3853–3864.

Fuller, R. M., Smith, G. M., Sanderson, J. M., Hill, R. A., Thomson, A. G., Cox, R., Brown, N. J., Clarke, R. T., Rothery, P., & Gerard, F. (2002). Land Cover Map 2000: A Guide to the Classification System. *Countryside Survey 2000 Module 7, Final Report*.

Gerard, F., et al. (2010). Land cover change in Europe between 1950 and 2000 determined employing aerial photography. *Progress in Physical Geography*, *34*, 183–205.

Han, W. S., & Burian, S. J. (2009). Determining effective impervious area for urban hydrologic modeling. *Journal of Hydrologic Engineering*, *14*, 111–120.

Haralick, R. M., Shanmugan, K., & Dinstein, I. (1973). Textural features for image classification. *IEEE Transactions on Systems, Man, and Cybernetics, 3*, 610–621.

Herold, M., Liu, X., & Clarke, K. C. (2003). Spatial metrics and image texture for mapping urban land use. *Photogrammetric Engineering & Remote Sensing, 69*, 991–1001.

Hooftman, D. & Bullock, J. (2012). Mapping to inform conservation: A case study of changes in semi-natural habitats and their connectivity over 70 years. *Biological Conservation, 145*, 30–38.

Hurd, J. D., & Civco, D. L. (2004). Temporal characterization of impervious surfaces for the State of Connecticut. *ASPRS Annual Conference Proceedings, Denver, Colorado, May 2004*.

Im, J., Lu, Z., Rhee, J., & Quackenbush, L. J. (2012). Impervious surface quantification using a synthesis of artificial immune networks and decision/regression trees from multi-sensor data. *Remote Sensing of Environment*, *117*, 102–113.

Institute of Hydrology. (1999). *Flood Estimation Handbook* (five volumes). Centre for Ecology and Hydrology, Oxfordshire, UK.

Kidd, C. H. R., & Lowing, M. J. (1979). The Wallingford urban subcacthment model. *Institute of Hydrology, Report No 60*. Wallingford, Oxfordshire, UK.

Landis, J. R., & Koch, G. G. (1977). The measurement of observer agreement for categorical data. *Biometrics, 33*, 159–174.

Lu D., Weng, Q., & Li, G. (2006). Residential population estimation using a remote sensing derived impervious surface approach. *International Journal of Remote Sensing, 27*, 3553–3570.

Lu D., Moran, E., & Hetrick, S. (2011). Detection of impervious surface change with multitemporal Landsat images in an urban–rural frontier. *ISPRS Journal of Photogrammetry and Remote Sensing, 66*, 298–306.

Morton, D., Rowland, C., Wood, L., Meek, C., Marston, C., Smith, G., Wadsworth, R., & Simpson, I.C. (2011). Final report for LCM2007 – the new UK land cover map. Countryside Survey Technical Report No 11/07 NERC/Centre for Ecology & Hydrology, 112.

Ogden, F. L., Pradhan, N. R., Downer, C. W., Zahner, J. A. (2011) Relative importance of impervious area, drainage density, width function, and subsurface storm drainage on flood runoff from an urbanized catchment. *Water Resources Research, 47*, W12503.

Pacifici, F., Chini, M., & Emery, W. J. (2009). A neural network approach using multi-scale textural metrics from very high-resolution panchromatic imagery for urban land-use classification. *Remote Sensing of Environment, 113*, 1276–1292.

Packman, J. (1980). The effects of urbanisation on flood magnitude and frequency. *Institute of Hydrology Report No 63,* Wallingford, Oxfordshire.

Perry, T., & Nawaz, R. (2008). An investigation into the extent and impacts of hard surfacing of domestic gardens in an area of Leeds, United Kingdom. *Landscape and Urban Planning, 86*, 1–13.

Richards, J. A., & Jia, X. (2006). *Remote Sensing Digital Image Analysis, Fourth edition.* Berlin: Springer-Verlag, pp. 232–242.

Schueler, T. R. (1994). The Importance of Imperviousness. *Watershed Protection Techniques, 1*, 100–111.

Shuster, W. D., Bonta, J., Thurston, H., Warnemuende, E., & Smith, D. R. (2005). Impact of impervious Surface on Watershed Hydrology. *Urban Water Journal*, *2*, 263–75.

Tavares, A. O., Pato, R. L., & Magalhães, M. C. (2012). Spatial and temporal land use change and occupation over the last half century in a peri-urban area. *Applied Geography*, *34*, 432–444.

Van de Voorde, T., De Genst, W., Canters, F., Stephenne, N., Wolff, E., & Binnard, M. (2003). Extraction of land use/land cover — Related information from very high resolution data in urban and suburban areas. *Proceedings of the 23rd Symposium of the European Association of Remote Sensing Laboratories* (pp. 237–244).

Van de Voorde, T., Jacquet, W., & Canters, F. (2011). Mapping form and function in urban areas: An approach based on urban metrics and continuous impervious surface data. *Landscape and Urban Planning*, *102*, 143–155.

Villarini, G., Smith, J.a., Serinaldi, F., Bales, J., Bates, P.D., & Krajewski, W.F. (2009). Flood frequency analysis for nonstationary annual peak records in an urban drainage basin. *Advances in Water Resources*, *32*, 1255–1266.

Verbeiren, B., Van De Voorde, T., Canters, F., Binard, M., Cornet, Y., Batelaan, O. (2013). Assessing urbanisation effects on rainfall-runoff using a remote sensing supported modelling strategy. *International Journal of Applied Earth Observation and Geoinformation*, *21*, 92–102.

Vogel, R.M., Yaindl, C., & Walter, M. (2011). Nonstationarity: Flood Magnification and Recurrence Reduction Factors in the United States. *JAWRA Journal of the American Water Resources Association*, *47*, 464–474.

Weng, Q. (2012). Remote sensing of impervious surfaces in the urban areas: Requirements, methods, and trends. *Remote Sensing of Environment*, *117*, 34–49.

Yuan, F., & Bauer, M. E. (2006). Mapping impervious surface area using high resolution imagery: A comparison of object-based and per pixel classification. *American Society for Photogrammetry and Remote Sensing Annual Conference Proceedings, Reno, Nevada, 2006*.

Zhou, Y. Y., & Wang, Y. Q. (2008). Extraction of impervious, surface areas from high spatial resolution imagery by multiple agent segmentation and classification. *Photogrammetric Engineering and Remote Sensing*, *74*, 857–868.